

This article was downloaded by:

On: 14 January 2011

Access details: Access Details: Free Access

Publisher Taylor & Francis

Informa Ltd Registered in England and Wales Registered Number: 1072954 Registered office: Mortimer House, 37-41 Mortimer Street, London W1T 3JH, UK



Molecular Simulation

Publication details, including instructions for authors and subscription information:

<http://www.informaworld.com/smpp/title~content=t713644482>

Graph theoretical approach to the mechanical strength of polymers

G. Gündüz^a; M. Dernaika^a; G. Dikencik^a; M. Fares^b; L. Aras^b

^a Kimya Mühendisliği Bölümü, Orta Doğu Teknik Üniversitesi, Ankara, Turkey

^b Kimya Bölümü, Orta Doğu Teknik Üniversitesi, Ankara, Turkey

id="ILM0002" data-bbox="278 294 350 308" style="font-family: serif;">$\frac{1}{2}$
file="GMOS_A_287007_O_XML_IMAGES/GMOS_A_287007_O_ILM0002.gif" data-bbox="278 308 880 322" style="font-family: serif;">$\frac{1}{2}$
id="ILM0003" data-bbox="278 322 350 336" style="font-family: serif;">$\frac{1}{2}$
file="GMOS_A_287007_O_XML_IMAGES/GMOS_A_287007_O_ILM0003.gif" data-bbox="278 336 880 350" style="font-family: serif;">$\frac{1}{2}$

To cite this Article Gündüz, G. , Dernaika, M. , Dikencik, G. , Fares, M. and Aras, L.(2008) 'Graph theoretical approach to the mechanical strength of polymers', *Molecular Simulation*, 34: 5, 541 – 558

To link to this Article: DOI: 10.1080/08927020701868367

URL: <http://dx.doi.org/10.1080/08927020701868367>

PLEASE SCROLL DOWN FOR ARTICLE

Full terms and conditions of use: <http://www.informaworld.com/terms-and-conditions-of-access.pdf>

This article may be used for research, teaching and private study purposes. Any substantial or systematic reproduction, re-distribution, re-selling, loan or sub-licensing, systematic supply or distribution in any form to anyone is expressly forbidden.

The publisher does not give any warranty express or implied or make any representation that the contents will be complete or accurate or up to date. The accuracy of any instructions, formulae and drug doses should be independently verified with primary sources. The publisher shall not be liable for any loss, actions, claims, proceedings, demand or costs or damages whatsoever or howsoever caused arising directly or indirectly in connection with or arising out of the use of this material.

Graph theoretical approach to the mechanical strength of polymers

G. Gündüz^{a*}, M. Dernaika^a, G. Dikencik^a, M. Fares^b and L. Aras^b

^aKimya Mühendisliği Bölümü, Orta Doğu Teknik Üniversitesi, Ankara 06531, Turkey; ^bKimya Bölümü, Orta Doğu Teknik Üniversitesi, Ankara 06531, Turkey

(Received 31 July 2007; final version received 4 December 2007)

In this research work, a graph theoretical approach has been introduced to find a mathematical model for the change of hardness of weakly cross-linked polymer network systems with the change of configurations. The polymers studied are (i) poly(methyl methacrylate), (ii) styrene–acrylonitrile copolymer and (iii) polystyrene. In very weakly cross-linked polymer network systems, both the chain entanglement and the network rigidity competitively contribute to the hardness of polymer network. The average length (i.e. molecular weight), and length distribution of chains between the cross-linking sites both play important roles in network rigidity. The former can be changed by the mole fraction of the cross-linker, and the latter by the molecular weight of the prepolymer formed, which can be controlled by the late addition of the cross-linker. Graph theoretical approach introduces simplifications to the dynamics of polymer chains and polymer network, and thus can explain the change of hardness with the change of chain statistics. It was shown that there was a very good agreement between the theoretical equations and the experimental hardness values of polymer network systems studied. It was also found that there were scaling relations between the parameters used in the theoretical equation.

Keywords: graph theory; polymer; hardness; mechanical strength; cross-linked; network

1. Introduction

The mechanical strengths of polymers depend on a number of different parameters. The molecular weight and its distribution, the functional groups on the polymer backbone, the chain conformation and configuration all have predominant roles in the mechanical properties of polymers. These parameters naturally affect the entanglements in thermoplastics and thus their mechanical properties. In thermosets, the degree of cross-linking has a primary influence on the mechanical properties. Although there is a vast literature on tensile, compressive and impact strengths of polymers and their dependences on the above-mentioned parameters the work on hardness is quite limited. Hardness represents the resistance to scratching, penetration, marring, etc. and at molecular level it is defined as the resistance to plastic deformation. The hardness of a polymer highly depends on the structure of the backbone and on the inter- and intra-chain weak forces. It also strongly depends on lattice distortions, lamellar thickness and lateral dimensions of paracrystals. In the literature, there has been numerous works in the past to explore the structure–property relations in polymers by using hardness test [1–9]. The dependence of hardness on crystallinity, molecular weight and blend composition were studied

[2,3,10–17]. The temperature dependence of hardness exhibits a very complex dynamics depending on the structure of polymer [16–19].

In the last two decades, there have been some efforts to use graph theory to make some models to explain the properties of polymers [20–26]. In the graph theory of polymers, ‘graph’ denotes the diagram of a chain structure, ‘vertices’ the submolecules and ‘edge’ the bond. The graph theory has been mostly utilised to classify the conformations of polymer chains and thus polymer structures [27–29]. The Wiener number, the complexity index, and the Kirchhoff matrix can be used to characterise the polymer conformations [30–32]. The theory finds applications not only in linear, cross-linked or branched polymers but also in gels, double-stranded conformations, telechelic molecules, dendrimers, hyperbranched polymers and composites [33–39].

Pleshakov studied the influence of network topology on the mechanical properties of polymers, and compared the long-term strengths of monofunctional and polyfunctional networks [40]. He found out that the long-term strengths of the polyfunctional polymer networks were some three- to four-fold of the long-term strengths of the monofunctional networks.

*Corresponding author. Email: ggunduz@metu.edu

The Rouse theory of viscoelasticity is closely related to the conformational statistics of Gaussian chains. Therefore, the graph theoretical approach can be used to solve the configurational properties of Gaussian chains. Yang pointed out that the Rouse and Zimm matrices in the molecular theory of polymer viscoelasticities are equivalent to the adjacency matrix and admittance (or Kirchhoff) matrix in graph theory, respectively [41]. He related the viscoelastic and conformational properties to the non-zero eigenvalues of the Zimm matrix. In order to solve the eigenvalue problems of Rouse and Zimm matrices, they are first represented by their corresponding eigen-graphs, which reflect the topological structure of the real chain.

The mechanical strength is a macro-level property; therefore, the graph theory has to be applied at macro-level. The 'graph' then denotes the macro-system where 'vertices' denote the entanglement points in linear polymers, and they denote the cross-linking sites in cross-linked polymers. The 'edges' then become either the chain lengths between the entanglement points, or the chain lengths between the cross-linking sites, respectively.

In amorphous polymers, the mechanical strength depends mostly on chain structures, their size distribution, and also on the extent of entanglement in thermoplastics or on the degree of cross-linking in thermosets. In a recent work, propylene glycol-based unsaturated polyester was modified with diphenylmethane-4,4'-diisocyanate, which leads to the formation of hybrid polymer network. It was found that the change of isocyanate/hydroxyl (NCO/OH) ratio affected the molecular dynamics of the polymers [42]. Therefore, the mechanical properties changed depending on the NCO/OH ratio. The change of toughness with NCO/OH ratio could be expressed by an equation known as logistic equation in nonlinear dynamics, such that,

$$K = \mu x(1 - x) + K_0, \quad (1)$$

where K_0 is the toughness of unmodified polyester and K is the toughness at any $x = \text{NCO/OH}$ molar ratio and μ is a constant. For the modified polymer, the change of the Young's modulus of compression (E_0) with NCO/OH, and also the change of yield strength (σ_y) with NCO/OH ratio both exhibited a Gaussian-like distribution with the same exponential coefficient, such that,

$$E = E_0 \exp(-3.5x^2), \quad (2)$$

$$\sigma_y = \sigma_0 \exp(-3.5x^2). \quad (3)$$

The equality of the exponential coefficients of the Gaussian distributions implies that the change of NCO/OH ratio influences both the elastic and plastic deformations differently but at the same proportion at all

NCO/OH ratios. In fact, there should be a linear dependence between E and σ_y . When the experimental data was plotted, it was observed that the graph of σ_y vs. E yielded a straight line [42]. Since toughness depends on elastic and plastic deformations, it was possible to express the change of toughness in terms of Young modulus in the form of a logistic equation. In other words, the toughness could be expressed in terms of yield strength and yield strength could be expressed in terms of Young modulus by a linear function [42]. The important point was that the mechanical property could be expressed in terms of mathematical functions in which the varying parameter was the molar ratio of the modifying species. In other words, the mechanical property was a smooth and analytic function of a molecular property which was the molar ratio in this case. It may be difficult to generalise this result to other cases if there is a severe change in the inner morphology of polymer such as phase separation or other heterogeneities. However, it was at least shown that the change of a mechanical property with respect to a change in the molar ratio of a component could be expressed by a mathematical function. This work showed that under certain conditions where the inner structure of the polymer represents a homogeneous structure without any grains or major defects the mechanical strengths of polymers can be explained entirely by chain dynamics or chain statistics.

The physical argument about the hardness of polymers is actually quite simple. The increase of entanglements of chains in linear polymers and the increase of the degree of cross-linking in thermoset polymers increases hardness. Let us consider the idealised network geometries seen in Figure 1.

The network *a* in Figure 1 is harder than the network *b* since the former has higher cross-linking density. In Figure 1, if the cross-linking sites analogically correspond to entanglement points in linear polymers, then *a* is harder than *b* since *a* is more rigid than *b* due to enhanced entanglement. However, such ideal same size loops as given in Figure 1(a) and (b) are not possible to achieve in polymers. Figure 1(c) represents a real situation where loops have varying sizes. In Figure 1(d), the sharp peak denotes the distribution of uniform size loops of Figure 1(a), while the broad peak denotes the distribution of the varying size loops of Figure 1(c).

How does the varying size distribution of loops affect the hardness of network, or, equivalently, how does the chain lengths between cross-linking sites in thermosets and chain lengths of segments between entanglement points in thermoplastics affect hardness? The statistics should affect hardness. In Figure 1(c), some loops are smaller and some are larger than the uniform size loops of Figure 1(a). In linear polymers, the entanglement density per unit volume levels off after certain molecular weight, therefore the hardness keeps almost constant for

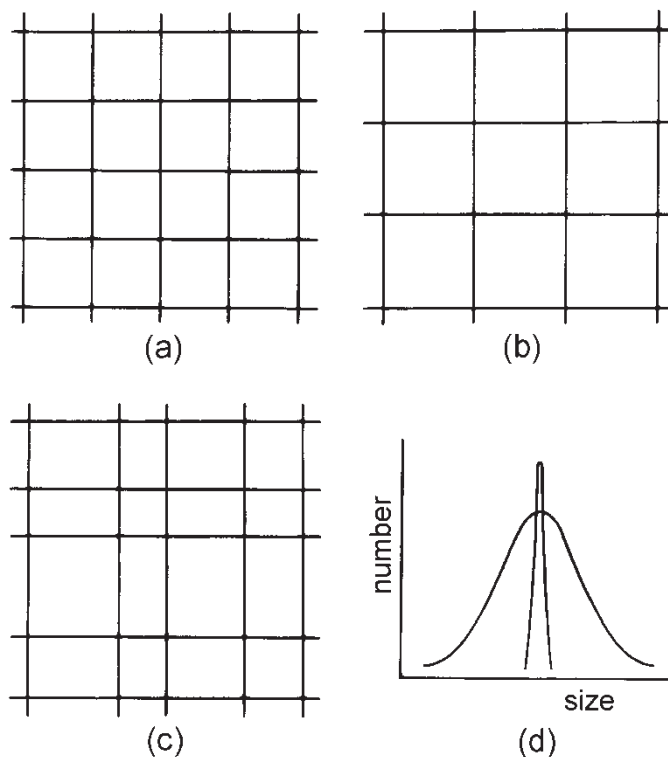


Figure 1. Networks and loop size distribution.

further increase of molecular weight. For a while, let us consider Figure 1(d) to represent two different molecular weight distributions of the same linear polymer where 'size' corresponds to 'molecular weight', and let us assume also that the narrow peak is at the region where entanglement density is reached to the saturation value where further increase of the molecular weight does not increase the hardness. Therefore, in the second case where the molecular weight distribution is broad, the molecules having larger lengths than the ones around the peak region do not contribute much to hardness. However, small size molecules are significant in number and they exhibit plastifying effect, and thus lower the hardness. Similarly, if Figure 1(a) and (c) represents cross-linked polymers, it is logical that the polymer represented by Figure 1(c) is softer than the polymer represented by Figure 1(a), because some of the relatively long chains present in Figure 1(c) lower the rigidity. From graph theoretical point of view, we can attribute some strength to each 'edge' between two subgroups, say simply between two carbon atoms or appropriate smallest units. The mechanical strength then becomes a function of these edge (or bond) energies as well as the density of entanglement points or cross-linking sites where an applied force is split into different directions. A similar situation occurs in network flow systems where the flow rate or current depends on the diameter of pipes and also on the number of branches at the junction points. The strong bond energy and the high entanglement or high

cross-linking density naturally yield higher mechanical strength, especially higher hardness. So the mechanical strength of the polymer shown by Figure 1(c) entirely depends on (i) the entanglement or cross-linking density and (ii) chain statistics between entanglement points or cross-linking sites. In this research work, three different polymers, which are, (i) poly(methyl methacrylate) (PMMA), (ii) styrene-acrylonitrile copolymer (SAC) and (iii) polystyrene (PS) were studied. As will be discussed below each has different microstructures. PMMA is purely amorphous, SAC has side group interactions, and PS has low crystallinity.

2. Mathematical modelling

If the length distribution of chains between cross-linking sites could be determined, then it might be possible to express hardness in terms of this distribution. There is almost no possibility to measure the length of these chains experimentally with the present techniques. In addition, it is usually very difficult to change the chain length distribution without changing the cross-linking density. New polymerisation procedure has to be adopted in order to alter the chain distribution. The chain length distribution can be altered by late addition of the cross-linker. We can find a mathematical relation between the lengths of the already formed linear chains just at the time of the addition of the cross-linker (e.g. of prepolymer)

and the lengths of chains between cross-linking sites in the network formed. The change in the physical and the mechanical properties can then be related to the chain length (i.e. molecular weight) of the prepolymer. The analysis of this system is quite complex but can be handled anyway. The theoretical treatment was given in a former work [43]; however, a better derivation of the mathematical relation was given in Appendix A. In order to see the effect of both the cross-linking density and the chain length distribution between the cross-linking sites, the cross-linker was used at very low concentrations. As explained in Appendix A, there are three important parameters which influence the molecular weight of a polymer in radical polymerisation of vinyl monomers. These are (i) the decay rate constant of the initiator, (ii) the polymerisation rate constants which influence the monomer concentration M and (iii) the different reactivity of the cross-linker than the monomer reactivity. In the course of polymerisation, the chain termination by disproportionation results in two chains; one is a dead chain and the other inactive chain with a vinyl end group. The inactive chain gets involved in further polymerisation reactions resulting in branched chains with large chain lengths. Therefore, the increase of the molecular weight of polymers is expected to increase in time in radical polymerisation reactions which can terminate by disproportionation. In addition, auto-acceleration reactions occurring in late periods also increase the molecular weight. In order to check the validity of this argument, the change of the molecular weight of the polymers studied in this research were plotted with respect to time of polymerisation in Figure A-1 in the Appendix A. So the distribution of chain lengths between the cross-linking sites was changed by adding the cross-linker at different times after the start of polymerisation.

The late addition of cross-linker however introduces two different structures to the system. The polymer formed after the addition of the cross-linker will be essentially a network polymer. Since some linear chains had already formed before the addition of the cross-linker, we then have a kind of interpenetrating polymer system where linear chains and the network coexist. As mentioned earlier branches also exist on the backbone. A sketch of such configuration was given in Figure 2.

Therefore, both the rigidity of the network and the extent of the entanglement of linear chains with each other and also with the network contribute to the hardness of the system. It was shown in Appendix A that the hardness of the interpenetrated system is given by Equation (A-35),

$$H = h_0 + h(kM)(kM - 1)(1 - C)^{kM-2}C^2, \quad (4)$$

where H is the hardness of the system, h_0 is the hardness for the case when the cross-linker is added just at the very

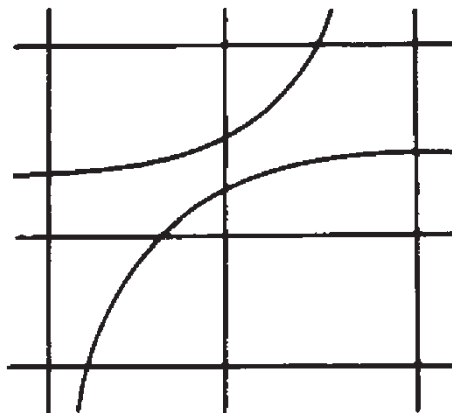


Figure 2. Interpenetrated system.

beginning, M is the molecular weight of the polymer (or prepolymer) just at the time of addition of the cross-linker and C is the mole fraction of the cross-linker. The constant h is a coefficient for the contribution of the probability distribution function (i.e. Equation (A-32)) to hardness. The constant k relates the molecular weight of the prepolymer to other chain lengths involved in polymerisation (see Equations (A-20)–(A-27) and (A-31)). The contribution of both linear chains and the chains of the weakly cross-linked network contribute to hardness in appropriate proportions according to graph theory, because, hardness depends on bond energy, entanglement and cross-linking density. The bond energy is an inherent property of monomers used in polymerisation, while entanglement and cross-linking density influence the system in proportion to chain length distribution which is a function of M and C , and given by Equation (A-32).

3. Experimental

Three different network structures were studied in this research. These polymers are (i) PMMA, (ii) SAC and (iii) PS. In the first system, methyl methacrylate (MMA) monomer was cross-linked with ethylene glycol dimethyl methacrylate (EGDM), while divinyl benzene (DVB) was used in 'ii' and 'iii'.

PMMA is amorphous, so Equation (4) can be easily applied for the change of hardness. In the copolymer system (e.g. SAC), the phenyl and nitrile side groups introduces additional effects to the cohesion of the chains, and this effect has to be introduced into the theoretical equation. In PS some small crystallinity showed up in the final product, and its effect also has to be included in the model.

It is known from the literature that the reactivities of acrylonitrile and styrene radicals towards their monomers are not the same; SAC compositions are different from their monomer compositions [44,45]. The disparity

of reactivity ratios introduces an unequal insertion rate of monomers into the copolymer. In order to have uniform distribution of acrylonitrile and styrene on the backbone of SAC, the azeotropic composition with 25% acrylonitrile and 75% styrene was used.

The monomers were purified from their inhibitors and the polymerisation reaction was carried in tubes by using dibenzoyl peroxide (DBP) as initiator. The tubes were closed and immersed into a constant temperature water bath shaker. MMA was polymerised at 50°C by using 0.5% DBP, styrene–acrylonitrile co-monomer (SA) at 57°C by using 0.06% DBP and styrene at 60°C by using 0.5% DBP. Three millilitres of prepolymer solution was taken from a tube just before the addition of the cross-linker and transferred onto methanol to remove soluble monomers. Just at this point the cross-linker was added into the tube. The cross-linker was injected into the tube by a micropipette. The weight-average molecular weights of the prepolymers were determined by viscometric methods utilising the constants given in the literature for Mark–Houwink–Sakurada equation [46,47]. The typical changes of the molecular weights were shown in Figure A-1. The molecular weight of the prepolymer in every tube was determined before the addition of the cross-linker.

The mole fractions of EGDM used for cross-linking MMA were 0.002, 0.004 and 0.005. The mole fractions of DVB used for cross-linking SA were 0.00066, 0.00110 and 0.00330. In cross-linking pure styrene, the fractions of DVB used were 0.000066, 0.000022, 0.000044 and 0.000066. We need to use such low concentrations in order to investigate the effect of chain statistics in the competitive effects of entanglement and network rigidity, and thus to investigate resulting scaled behaviour of the network. At high concentrations of the cross-linker, the network rigidity predominates and the influence of chain statistics cannot be observed.

After the addition of the cross-linker, the tubes were kept in a water-bath for one day. The solid polymer samples were taken out by breaking away the glass tubes. The samples were kept in a drier for another 3 days to drive off all the monomers, meanwhile, the temperature was raised from 60 to 80°C gradually.

Hardness tests were carried by using (i) Brinell Hardness method (ISO 2039-73; Instrument: Heckert HPO 250 – CMEA PC 501-66) and (ii) Shore D (ASTM D2240) durometer test, (Instrument: Rex Durometer model: 1700). The Shore D durometer was easy to use and it was especially preferred to determine the change of hardness with temperature [48]. Both techniques yielded similar results. A linear expression was obtained between Brinell hardness number (BHN) and Shore D value, such that,

$$\text{BHN} = 0.2425 \times \text{Shore D} - 0.65. \quad (5)$$

It is seen that BHN and Shore D are convertible to each other.

The hardness values shown in the figures were found out from the average of 10 tests; the standard deviation was usually less than 0.5%.

Nicolet Fourier Infrared Spectrometer (510) was used for the Fourier Transform Infra Red (FTIR) spectrum of SAC samples, and IR OMNIC software was used to trace the sensitive change in nitrile group frequency. Huber X-ray diffractometer with Cu K α radiation was used to determine the crystallinity in PS specimens.

3.1 Poly(methyl methacrylate)

The change of hardness of PMMA at different molecular weights of the prepolymer for different mole fractions of the cross-linker is shown in Figure 3.

In all cases, hardness increases first, passes through a maximum, and then declines. At the very early addition of the cross-linker, the network structure would have relatively smaller chain lengths between the cross-linking sites in the early stages of polymerisation and they would increase towards the end of polymerisation. The loops formed from long chains naturally introduce a kind of soft regions to the network resulting in a decrease in the hardness. At very late addition of the cross-linker, there would be a large amount of linear chains formed which also decreases hardness.

In Figure 3, the points are experimental values, and the solid curves are the predictions of Equation (4). The solid curves are obtained from nonlinear regression analysis. It is seen that there is a very good agreement between the experimental values and the prediction of Equation (4). The values of h and k are given in Table 1.

The proportionality constant h is fixed for all mole fractions of the cross-linker used, and the change of k with cross-linker mole fraction was calculated. h indicates the coefficient of contribution of chain distribution effect to hardness. The constant value of h for all cases indicates that the bond energy does not

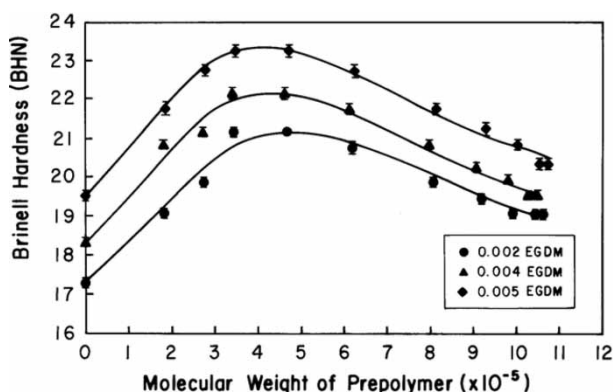


Figure 3. Change of hardness of PMMA network with the molecular weight of prepolymer.

Table 1. Different calculated parameters of Equation (4) for PMMA network.

C^a	h	k	$MW_{\max} \times 10^{-5}$
0.002	7.1	0.002095	4.771
0.004	7.1	0.001161	4.290
0.005	7.1	0.000973	4.108

^a Mole fraction.

change due to configuration, therefore the graph theoretical approach can be successfully used.

Table 1 shows that k value decreases as the mole fraction of the cross-linker increases. This is because the effect of the chain distribution on hardness decreases as C increases as it is also seen from Equation (4). That is, $(1 - C)^{kM-2}$ term overwhelms C^2 term in Equation (4) as C increases. At large C values, the influence of the second term on the right of Equation (4) must have no significant contribution.

The MW_{\max} term in the last column of Table 1 denotes the molecular weight of the prepolymer where the maximum hardness is achieved. It also decreases with the increase of C .

3.2 Styrene–acrylonitrile copolymer

The change of hardness with the molecular weight of the prepolymer for styrene–acrylonitrile co-monomer is shown in Figure 4.

The hardness somehow oscillates in Figure 4. The hardness first increases as the cross-linker concentration increases as also in Figure 3. SAC carry both nitrile ($-\text{CN}$) and phenyl side groups on the backbone. These groups are involved in weak interactions as seen in Figure 5.

The ability of the chains to bend, stretch or to undergo different chain motions decreases as network rigidity increases. Therefore, the chain entanglement

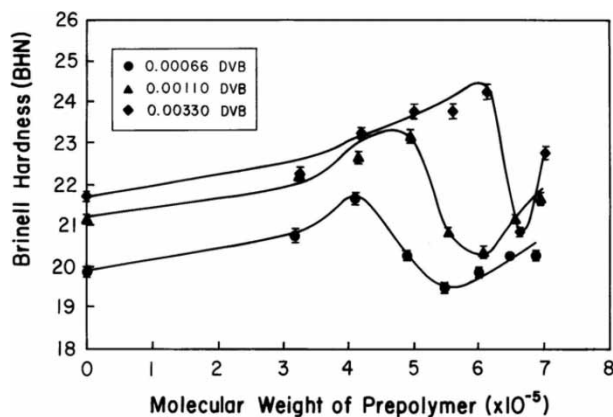


Figure 4. Change of hardness of SAC network with the molecular weight of prepolymer.

in the weakly cross-linked network decreases. Thus, the interactions between side groups such as nitrile–nitrile attractions on adjacent chains and phenyl–nitrile attractions on the same chain decrease. In other words, the change in the extent of nitrile–nitrile and phenyl–nitrile interactions causes a change also in the hardness of SAC network. This was not a case with PMMA because it is a homopolymer, and the change in the interactions of ester side chain correlates in proportion with other changes, and they are all absorbed by the constant h in Equation (4). However, in the case of SAC network the change in the extent of interactions of the side groups have to be included in Equation (4).

Since hardness directly depends on the probability distribution (i.e. Equations (A-32) and (A-33)), the extent of interactions of the side groups also depends on the same probability distribution according to graph theoretical considerations as discussed above. Since the proportion of phenyl–nitrile and nitrile–nitrile interactions are influenced by the same probability distribution we can express one in terms of the other. In acrylonitrile polymers, some nitrile groups ($-\text{CN}$) are potentially available for intermolecular dipolar bonding [49]. Saum [50] showed that there exist strong intermolecular forces in polyacrylonitrile and arise principally from dipole–dipole interactions between $-\text{CN}$ groups on adjacent chains. Another study showed that the high polarity of nitrile groups in the polymer causes the formation of numerous intermolecular hydrogen bonds between the chains [51].

As the nitrile-stretching mode is well isolated in frequency and it is not coupled with other molecular motions, it can be considered as a pure stretching frequency. The side group interactions can be taken into account by the frequency shifts in the nitrile groups [52].

The influence of the side group interactions can be introduced into Equation (4) by measuring the extent of this interaction, which, can be determined from FTIR spectrum. The change in the nitrile ($-\text{CN}$) frequency shift

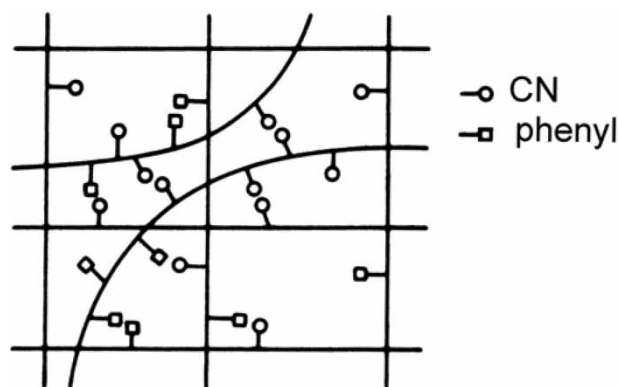


Figure 5. Interpenetrated system with side group interactions.

gives an idea about how the vibrations are affected by the mutual interactions of nitrile groups. The interaction of a $-\text{CN}$ group by another one increases stretching so the energy and thus frequency associated with it increases. An increase in the frequency denotes higher distortion and repositioning of the groups. The close $-\text{CN}$ groups yield more compact network and thus higher hardness. Therefore, the shift in the frequency of vibration is a kind of measure of the influence of side groups on hardness. Since the side group interactions are controlled by the structure of the loop sizes and the distribution of chains between the cross-linking sites, we can express the increase in the hardness in terms of Equation (4). Hence, we can write,

$$\Delta H_s = h\varepsilon\nu(kM)(kM - 1)(1 - C)^{kM-2}C^2, \quad (6)$$

where ν is the frequency of vibration of dipole–dipole interactions of nitrile groups, and ε is a coefficient that converts the side group interactions into hardness. ΔH_s , which is the contribution of side group interactions on hardness can be simply added to Equation (4), such that,

$$H = h_0 + h(kM)(kM - 1)(1 - C)^{kM-2}C^2(1 + \varepsilon\nu). \quad (7)$$

The frequency ν was determined from the FTIR spectrum of each cross-linked SAC, and different frequencies were obtained for different networks. The measured frequency values of nitrile group interactions at different cross-linker mole fractions are tabulated in Table 2 with respect to the molecular weight of the prepolymer. As additional information, the measured hardness values are also tabulated in the last column.

The hardness of SAC network first increases and then declines to a minimum as seen from Figure 4. The molecular weight of the prepolymer increases causing a more uniform and narrower loop size distribution, which, in turn, increases overall network rigidity, and thus hardness until the maximum point is reached. The frequency of $-\text{CN}$ stretching decreases in the first three data in $\text{DVB} = 0.00066$ case, in the first four data in $\text{DVB} = 0.00110$ case and in the first six data in $\text{DVB} = 0.00330$ case. The increased concentration of the cross-linker decreases the loop sizes and thus restricts the vibrational motion of the nitrile groups. Although the increase of the molecular weight of the prepolymer increases the loop sizes, at high cross-linker concentrations the loop sizes get smaller, and the vibrations of nitrile groups are restricted even at higher molecular weight of the prepolymer.

In Figure 4, the hardness starts to increase again after reaching a minimum value. In this case, the network rigidity due to uniform distribution of loops is quite lost, and the chain entanglement is increased significantly. It, in turn, results in closer packing of chains. The increased

Table 2. The frequency of nitrile group interactions in different networks.

MW of prepolymer ($\times 10^{-5}$)	Frequency (cm^{-1})	Hardness (BHN)
DVB = 0.00066		
0 ^a	2241.21	19.86
3.19	2238.07	20.75
4.10	2233.59	21.65
4.89	2237.66	20.26
5.48	2243.51	19.46
6.00	2242.98	19.86
6.48	2237.23	20.26
6.87	2236.10	20.26
DVB = 0.00110		
0	2235.17	21.18
3.23	2234.42	22.18
4.15	2231.34	22.65
4.95	2228.78	23.15
5.54	2238.12	20.84
6.07	2241.28	20.35
6.56	2234.36	21.18
6.95	2232.82	21.65
DVB = 0.00330		
0	2234.69	21.73
3.26	2233.28	22.25
4.20	2231.62	23.23
5.01	2230.16	23.76
5.61	2228.82	23.76
6.14	2226.47	24.24
6.64	2236.72	20.84
7.03	2229.23	22.75

^a MW = 0 means there is no prepolymer (i.e. the very beginning).

chain entanglement causes an increase in hardness again. Besides, the nitrile–nitrile interaction can increase the nitrile group stretching, which, in turn, increases frequency. Although the stretchings increase in the network, the effect of increased entanglement overwhelms and hardness keeps increasing.

It is seen from Figure 4 that as the amount of the cross-linker concentration increases (i.e. from 0.00066 to 0.0033 mole fraction) the curves shift upwards. This is because of the higher cross-linker mole fractions imparting higher rigidities. Besides, as the cross-linker mole fraction increases curves shift right. In PMMA case they shifted to the left. The behaviour in the case of SAC network can be explained in terms of the side group interactions as explained above.

In Figure 4, the points are experimental values. The solid curves were obtained from Equation (7) by nonlinear regression analysis. There is a very good agreement between experimental points and the prediction of Equation (7). The value of ε was found to be -0.000447 .

The changes of h and k values for the curves seen in Figure 4 are given in Table 3.

The constant ε which denotes the contribution of frequency shift to hardness came out to be negative

Table 3. The determined parameters of Equation (7) for SAC network.

C^a	h	k	ε	$MW_{\max} \times 10^{-5}$
0.00066	2943	0.0160	-0.000447	4.05
0.00110	2943	0.0085	-0.000447	4.85
0.00330	2943	0.0021	-0.000447	6.10

^a Mole fraction.

in sign, because the increase in frequency is due to decline in the entanglements and/or network rigidity so that nitrile groups can stretch farther yielding an increase in the frequency. So the frequency increase implies a negative effect on hardness.

3.3 Polystyrene

The change of hardness of PS network is shown in Figure 6. The hardness increases first, passes through a maximum, and then declines as in the case of PMMA. The curves shift to the left and upward as the concentration of the cross-linker decreases. In other words, the hardness tends to decrease with the increase of the mole fraction of the cross-linker in the range $C = 0.0000066$ – 0.000066 .

This fact seems to be in contradiction with what is known in the literature such that hardness increases with the concentration of the cross-linker. However, the cross-linker concentrations used in the literature are several orders larger than the ones used in this research. In linear polymers, the hardness increases with the number density of entanglements (i.e. number of entanglements per unit volume of polymer), while in cross-linked polymers the hardness increases with the network rigidity or with the number density of cross-linking sites per unit volume. The molar fraction of the cross-linker used in this research has such a low value (i.e. $C = 0.0000066$ – 0.000066) that the cross-linking reduces the number of entanglements lowering the hardness due to entanglement yet the cross-linker concentration is so low that

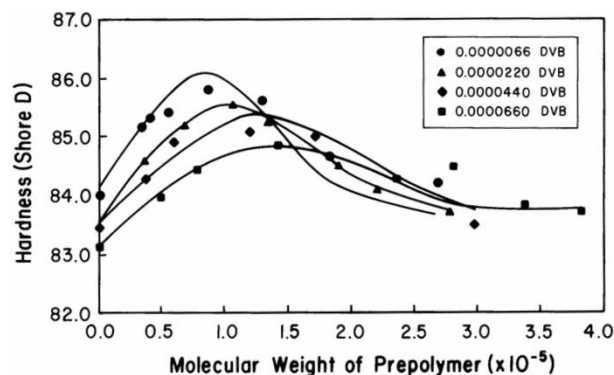


Figure 6. Change of hardness of PS network with the molecular weight of prepolymer.

it cannot sufficiently impart network rigidity. A similar result was obtained also with PMMA in a former work where the values of C were about 200–500 times less than the ones used here [43]. So both the chain entanglement and the network rigidity contribute to the hardness of the very weakly cross-linked systems. If the cross-linker concentration is decreased to extremely low values such that the entanglement density is not influenced significantly but there is some contribution to the network rigidity, then the hardness is expected again to increase with the amount of the cross-linker [43]. Therefore, the very little amount of additions of the cross-linker can be used as a technique to enlighten the inner structure of network polymers as the chain configuration and the resulting mechanical properties are concerned.

The entanglement in polymers is due to the natural fact that the material tends to occupy minimum volume. If the conformations of polymer chains are such that the minimum volume can be achieved through close packing of the chains then chain alignment or crystallinity can take place in the polymer. Entanglement and crystallinity are two competitive phenomena to achieve minimum volume of packing; one occurs at the expense of the other. In very weakly cross-linked polymers, the entanglement is reduced. The chains then may intend to achieve minimum volume through crystallinity. The X-ray Diffraction (XRD) spectrum of PMMA and SAC network did not show any crystallinity. In the case of PS, crystallinity was observed in late addition of the cross-linker. This was an interesting observation, because PS has a tendency to crystallise and it was stimulated by the late addition of the cross-linker. A sample XRD spectrum is shown in Figure 7.

It is seen from Table 4 that the chain alignment or crystallinity does not take place at early additions of the cross-linker. The first two data in each set in Table 4 refer to the cross-linker additions at $t = 0$ and 0.5 h, respectively. It is seen that there is no crystallinity occurring for these cases. For the set $C = 0.0000066$, the addition at $t = 2$ h, which refers to the third data also displays no crystallinity. The last data in each set refer to the addition of the cross-linker at $t = 17$ h, and no chain alignment occurs for this case either. In other words, at very early and very late additions of the cross-linker, no crystallinity was observed in specimens. The uniformity of loop size distribution, the number density of linear dead chains and the number of branchings favour the chain alignment in some way at moderately late additions of the cross-linker. However, a detailed analysis needs to be made to understand how it happens.

Since the crystallinity is caused by the resulting structure of the network, which is, in fact, a function of the molecular weight of the prepolymer and the concentration of the cross-linker, the hardness can

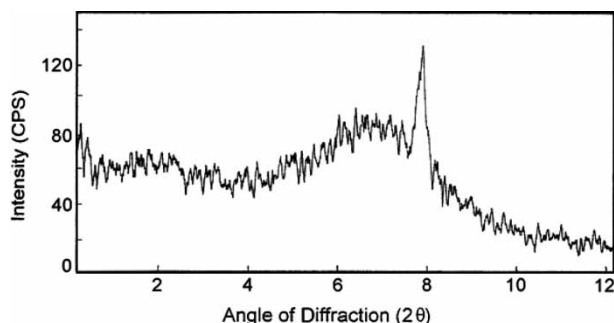


Figure 7. The XRD pattern of a weakly cross-linked PS network formed from the late addition of the cross-linker.

be expressed by an equation similar to Equation (7), such that,

$$H = h_0 + h(kM)(kM - 1)(1 - C)^{kM-2}C^2(1 + g\rho), \quad (8)$$

where ρ denotes the percent crystallinity and g is a coefficient that accounts for the effect of crystallinity on hardness.

In Figure 6, the points are experimental values and the curves are the predictions of Equation (8) obtained by nonlinear regression analysis. There is a good agreement between the experimental points and the theoretical equation as in the case of PMMA and SAC network. Table 5 shows the values of the constants of Equation (8).

The value of g also decreases like that of k with the increase of the mole fraction of the cross-linker. The contribution of crystallinity to hardness decreases as the cross-linker concentration increases as expected.

4. Scaling relations

The derivation of Equations (A-32)–(A-35) was based on the concept that the time past until the addition of the cross-linker directly influences the molecular weight of the prepolymer, which, in turn, affects all the physical parameters such as the molecular weight of the chains between the cross-linking sites, the loop size distribution, the average loop size, the rigidity of the network, the size

Table 5. The determined parameters of Equation (8) for PS network.

C^a	h	k	g	$MW_{\max} \times 10^{-5}$
0.0000066	3	4.59	7.92	0.795
0.0000220	3	1.01	3.14	1.10
0.0000440	3	0.40	1.89	1.27
0.0000660	3	0.26	1.37	1.42

^a Mole fraction.

of the chains attached as branches at the network, the extent of entanglements of all chains at the weakly cross-linked network and also the entanglements of linear dead and inactive chains. However, all these variables nonlinearly correlate with each other and it is expected that one variable can be mathematically expressed in terms of the other variable. It is well known in nonlinear dynamics that such dependences can be expressed by means of a power law equation. According to graph theory, the correlated changes of parameters originate from the vertex–edge–complexity relations [53]. An observation that can be done from Figures 3, 4 and 6 is that the hardness exhibits a maximum at certain molecular weight of the prepolymer, and it shifts to higher or lower molecular weights of the prepolymer as the mole fraction of the cross-linker is changed. So it is likely that the molecular weight of the prepolymer that gives the maximum hardness displays a scaling relation with the mole fraction of the cross-linker. The molecular weight of the prepolymer that gives the maximum hardness (i.e. MW_{\max}) was determined and tabulated in Tables 1, 3, and 5 for PMMA, SAC and PS networks, respectively. The scaling relation can be expressed as,

$$MW_{\max} \sim C^\alpha, \quad (9)$$

where α is the scaling power.

The constant k determined from the data can also scale with C , such that,

$$k \sim C^\beta. \quad (10)$$

Table 4. The percentage alignment in PS at different mole fractions of DVB.

0.0000066		0.0000220		0.0000440		0.0000660	
$MW (\times 10^{-5})^a$	$\rho (\%)^b$	$MW (\times 10^{-5})$	$\rho (\%)$	$MW (\times 10^{-5})$	$\rho (\%)$	$MW (\times 10^{-5})$	$\rho (\%)$
0.33	0.00	0.36	0.00	0.375	0.00	0.40	0.00
0.40	0.00	0.49	0.00	0.60	0.00	0.685	0.00
0.55	0.00	0.68	2.45	1.20	6.53	1.42	3.60
0.90	3.00	1.05	10.4	1.72	8.40	1.81	1.78
1.29	4.82	1.34	3.30	2.36	9.74	2.58	2.15
1.83	7.36	2.21	7.42	2.45	11.0	2.83	0.78
2.69	0.00	2.78	0.00	2.98	0.00	3.04	0.00

^a Molecular weight of prepolymer. ^b Percent of crystallinity.

So it is likely that a similar relation exists between MW_{\max} and k ,

$$k \sim (MW_{\max})^{\gamma}. \quad (11)$$

In Equation (8), g looks like an arbitrary constant because it varies as seen from Table 5; and by using any g it may be possible to get a curve fit of Equation (8) to the experimental data. However, this is not the case in Equation (7) where ε is constant for all the mole fractions of the cross-linker used. In the case of Equation (8), g varied because crystalline regions stand as separate domains in the polymer, therefore, their contribution to hardness will not be constant at different molar fractions of the cross-linker as their number density and their size distributions would contribute in a different way to hardness. But we can say that since all variables are expected to correlate with each other g must also have a power law dependence on the variables C , MW_{\max} and k , such that,

$$g \sim C^{\mu}, \quad (12)$$

$$g \sim (MW_{\max})^{\nu}, \quad (13)$$

$$g \sim k^{\xi}. \quad (14)$$

If the existence of the relations given by Equations (12)–(14) can be experimentally verified then g is not an arbitrary constant at all but a parameter correlating with all other parameters of the network system.

The only experimental variable in Equations (9)–(14) is C . All the rest are determined quantities. The graphs of Equations (9)–(14) on ‘log–log’ scale were given for PS in Figure 8. The similar graphs of Equations (9)–(12) were obtained also for PMMA and SAC network, but they were not given here.

It is seen that in all cases a linear relation exists. This proves the existence of scaling relations between the variables of the weakly cross-linked network system. It, in fact, proves the fundamental assumption that all variables nonlinearly correlate during the evolution of the network which is a three dimensional graph. In addition we can also say that g is not an arbitrary constant, it does correlate with the variables of the system.

Therefore $g\rho$ term of Equation (8) can be now rewritten by using Equation (12) as,

$$g\rho = g'C^{\mu}\rho, \quad (15)$$

where g' is a simple constant. Thus Equation (8) becomes,

$$H = h_0 + h(kM)(kM - 1)(1 - C)^{kM-2}C^2(1 + g'C^{\mu}\rho), \quad (16)$$

where the independent variables are now only M and C .

The powers of the scaling equations can be easily determined from the slopes of ‘log–log’ plots. These values are tabulated in Table 6. α and β values came out to be same both for SAC and PS.

4.1 Combined scalings

The existence of the scaling relations among the parameters of the theoretical Equations (4), (7) and (8) implies that scaling relations can exist among the combined parameters also. By using Table 6, we obtain, For PMMA:

$$k \times MW_{\max} \sim C^{\alpha+\beta} \sim C^{-0.16-0.84} \sim C^{-1}. \quad (17)$$

For SAC:

$$k \times MW_{\max} \sim C^{\alpha+\beta} \sim C^{0.25-1.26} \sim C^{-1}.$$

For PS:

$$k \times MW_{\max} \sim C^{\alpha+\beta} \sim C^{0.25-1.26} \sim C^{-1},$$

$$g \times MW_{\max} \sim C^{\alpha+\mu} \sim C^{0.25-0.76} \sim C^{-0.5}, \quad (18)$$

$$k \times g \sim C^{\beta+\mu} \sim C^{-1.26-0.76} \sim C^{-2}. \quad (19)$$

The powers of combined scaling relations are ‘ -1 , ‘ -0.5 , and ‘ -2 ’ as seen from Equations (17)–(19). They are much simpler in numerical values than those numbers given in Table 6. This indicates that the nature of physical network formed can be understood by the concepts of graph theory.

Equation (17) holds for PMMA, SAC and PS network. It was shown to hold also at different molar fractions of PMMA and PS [43,54]. It seems to be a universal relation not depending on the type of polymer.

5. Conclusions

Graph theoretical approach to mechanical strength of polymers was discussed in this work, and it was shown that the change of hardness of weakly cross-linked polymers with the chain length distribution can be explained by theoretical equations. The following specific conclusions were obtained from the experimental results.

- (1) The hardness of the very weakly cross-linked network polymers by the late addition of the cross-linker depends on the molecular weight of the prepolymer at the time of the addition of the cross-linker. The hardness exhibits an asymmetric form for PMMA and PS, while it exhibits an oscillating form for SAC.
- (2) The change of hardness for amorphous PMMA can be described by a theoretical equation which is based

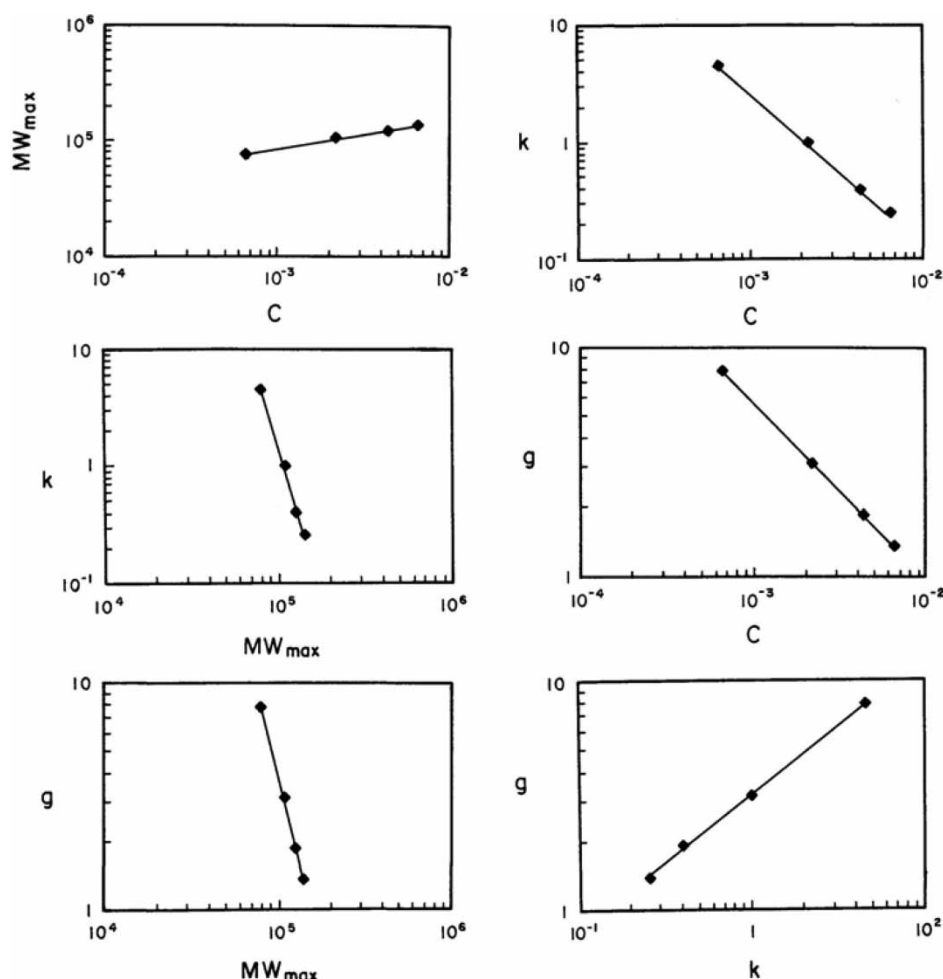


Figure 8. Scaling relations in PS.

on chain statistics (i.e. Equation (A-32)). The independent variables of the probability equation are the molecular weight of the prepolymer, and the molar fraction of the cross-linker.

- (3) The theoretical equation can be modified for the interactions of the side groups on the backbone for SAC. The IR frequency of vibration of nitrile–nitrile interaction can be used to account for the side group interactions in the theoretical equation (i.e. Equation (7)) in terms of the probability distribution function.
- (4) The late addition of the cross-linker results in chain alignment or crystallinity in PS, and its influence can

be incorporated into the theoretical equation in terms of the probability distribution function.

- (5) The parameters influencing the chain statistics and thus the structure of the network evolved all correlate with each other displaying scaling relations. The scaling relations exist between C , MW_{\max} , k , and g .
- (6) The combined scaling relations exhibited simple forms such that, $k \times MW_{\max} \sim C^{-1}$, $g \times MW_{\max} \sim C^{-0.5}$ and $k \times g \sim C^{-2}$. Such simplicity inspires that there may exist some simple mechanisms to explain the relation between chain statistics and the mechanical strength by using graph theory.
- (7) The relation $k \times MW_{\max} \sim C^{-1}$ holds for all polymer network systems, so it seems to be a universal relation.

Table 6. The values of scaling powers for the polymer networks.

Power	α	β	γ	μ	ν	ξ
PMMA	-0.16	-0.84	5.21			
SAC	0.25	-1.26	-5.12			
PS	0.25	-1.26	-0.21	-0.76	-3.06	0.60

Acknowledgements

The authors appreciate Kâmil Alptekin for his technical drawing of some of the figures.

References

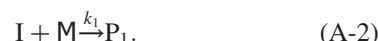
- [1] J.M. Salazar and F.J.B. Calleja, *Correlation of hardness and microstructure in unoriented lamellar polyethylene*, J. Mater. Sci. 18 (1983), pp. 1077–1082.
- [2] F.J.B. Calleja, D.R. Rueda, J. Garcia, F.P. Wolf, and V.H. Karl, *Influence of pressure and crystallization rate on the surface microhardness of high-density polyethylene*, J. Mater. Sci. 21 (1986), pp. 1139–1144.
- [3] J.M. Salazar, J.M.G. Tijero, and F.J.B. Calleja, *Microstructural changes in polyethylene-polypropylene blends as revealed by microhardness*, J. Mater. Sci. 23 (1988), pp. 862–866.
- [4] J. Slonecki, *Investigations of the hardness and thermal properties of copoly(ether-ester)s containing segments of different molecular weights*, Polymer 31 (1990), pp. 1464–1466.
- [5] D. Park, B. Kesler, V. Galiatsatos, and J.P. Kennedy, *Amphiphilic networks. XI. Mechanical properties and morphology*, J. Appl. Polym. Sci. 66 (1997), pp. 901–910.
- [6] S.K. Brauman, B.L. Myersacosta, P.C. Lokensgard, and M.M. Steiner, *Phenol/Cresol-formaldehyde resin characterization and contribution to product hardness*, Polym. Eng. Sci. 30 (1990), pp. 257–262.
- [7] I.M. Low, G. Paglia, and C. Shi, *Indentation responses of viscoelastic materials*, J. Appl. Polym. Sci. 70 (1998), pp. 2349–2352.
- [8] J.M. Salazar, J.C.C. Camara, E.L. Cabarcos, and F.J.B. Calleja, *Temperature dependence of microhardness in the 70/30 polyvinylidene fluoride-trifluorethylene copolymer: new structural aspects of the curie transition*, Colloid Polym. Sci. 266 (1988), pp. 41–45.
- [9] D.M. Shinozaki and A. Klauzner, *Stress relaxation of high impact polystyrene*, J. Mater. Sci. 26 (1991), pp. 5865–5872.
- [10] F.J.B. Calleja, L. Giri, I.M. Ward, and D.L.M. Cansfield, *Microstructure of bulk crystallized linear polyethylene: correlation of microhardness and yield*, J. Mater. Sci. 30 (1995), pp. 1139–1143.
- [11] R. Katara, R. Bajpai, and S.C. Datt, *Microhardness of blends of polystyrene and poly(methyl methacrylate)*, Polym. Test. 10 (1991), pp. 139–143.
- [12] M. Tasdemir, *Properties of acrylonitrile-butadiene-styrene/polycarbonate blends with styrene-butadiene-styrene block copolymer*, J. Appl. Polym. Sci. 93 (2004), pp. 2521–2527.
- [13] M. Begum and Siddaramaiah, *Synthesis and characterization of polyurethane/polybutyl methacrylate interpenetrating polymer networks*, J. Mater. Sci. 39(14) (2004), pp. 4615–4623.
- [14] B.K.K. Swamy, Siddaramaiah, H. Somashekarappa, and R. Somashekar, *Structure-property relationship in polyaniline-filled castor oil based chain extended polyurethanes*, Polym. Eng. Sci. 44(4) (2004), pp. 772–778.
- [15] F. Findik, M. Misirlioglu, and U. Soy, *The structural features of glass fibre reinforced polyester matrix composites*, Sci. Eng. Compos. Mater. 10(4) (2002), pp. 287–295.
- [16] S. Fakirov, F.J.B. Calleja, and M. Krumova, *On the relationship between microhardness and glass transition temperature of some amorphous polymers*, J. Polym. Sci. B: Polym. Phys. 37 (1999), pp. 1413–1419.
- [17] E. Vassileva, F.J.B. Calleja, M.E. Cagiao, and S. Fakirov, *Gelatin films with very high surface hardness*, Macromol. Rapid Commun. 19 (1998), pp. 451–454.
- [18] C.W. Bunn, *The melting points of chain polymers*, J. Polym. Sci. B: Polym. Sci. 34(5) (1996), pp. 799–819.
- [19] M.F. Mina, F. Ania, F.J.B. Calleja, and T. Asano, *Microhardness studies of PMMA/natural rubber blends*, J. Appl. Polym. Sci. 91 (2004), pp. 205–210.
- [20] Y.T. Yang and T. Yu, *Graph-theory of configurational and viscoelastic properties of polymers. 2. Linear polymer-chains containing small copolymer blocks*, Makromolekulare Chemie-Macromol. Chem. Phys. 187 (1986), pp. 441–454.
- [21] A.J. Polak and R.C. Sundahl, *Application of chemical graph theory for the estimation of polymer dielectric properties*, Polymer 30(7) (1989), pp. 1314–1318.
- [22] E. Buffet and J.V. Pule, *Polymers and random graphs*, J. Stat. Phys. 64 (1991), pp. 87–110.
- [23] B.G. Sumpter and D.W. Noid, *Neural networks and graph-theory as computational tools for predicting polymer properties*, Macromol. Theor. Simul. 3(2) (1994), pp. 363–378.
- [24] G. Wei, *Shapes and sizes of linear and circular multiple-ring macromolecules*, Polym. Adv. Technol. 8 (1997), pp. 265–269.
- [25] P. Licinio and A.V. Teixeira, *Relaxation of ideal polymer networks*, Philos. Mag. B 78(2) (1998), pp. 171–175.
- [26] S.I. Kuchanov, S.V. Korolev, and S.V. Panyukov, *Graphs in chemical physics of polymers*, in *Advances in Chemical Physics*, I. Prigogine and S.A. Rice, eds., Vol. 72, American Chemical Society, Washington, DC, 1988, pp. 115–326.
- [27] S.M. Patra and Vishveshwara, *Classification of polymer structures by graph theory*, Int. J. Quantum Chem. 71 (1999), pp. 349–356.
- [28] S. Higuchi, *Compact polymers on decorated square lattices*, J. Phys. A: Math. Gen. 32 (1999), pp. 3697–3709.
- [29] P.D. Iedema and H.C. J. Hoefsloot, *Synthesis of branched polymer architectures from molecular weight and branching distributions for radical polymerisation with long-chain branching, accounting for topology-controlled random scission*, Macromol. Theor. Simul. 10 (2001), pp. 855–869.
- [30] D. Bonchev, E.J. Markel, and A.H. Dekmezian, *Long chain branch polymer chain dimensions: application of topology to Zimm–Stockmayer model*, Polymer 43 (2002), pp. 203–222.
- [31] D. Bonchev, A.H. Dekmezian, E.J. Markel, and A. Faldi, *Topology-rheology regression models for monodisperse linear and branched polyethylenes*, J. Appl. Polym. Sci. 90 (2003), pp. 2648–2656.
- [32] D. Bonchev, *On the complexity of directed biological networks*, SAR QSAR Environ. Res. 14(3) (2003), pp. 199–214.
- [33] J. Bicerano, *Prediction of Polymer Properties*, Marcel Dekker, New York, NY, 1996.
- [34] C. Zhong and C. Yang, *Approach for the calculation of high-order connectivity indices of polymers and its application*, J. Polym. Sci. B: Polym. Phys. 40 (2002), pp. 401–407.
- [35] F. Liu, L. Dai, and Z. Yang, *Theory for the force-stretched double-stranded chain molecule*, J. Chem. Phys. 119(15) (2003), pp. 8112–8123.
- [36] Y.B. Raviv, T.M. Snyder, and Z.G. Wang, *Reversible association of telechelic molecules: an application of graph theory*, Langmuir 20 (2004), pp. 7860–7870.
- [37] B.E. Eichinger, *Embeddable random networks: method*, Polymer 46 (2005), pp. 4258–4264.
- [38] Y.Y. Li, Y.P. Han, Y.H. Zhao, and J. Sheng, *Study on phase formation and evolution of high impact polystyrene with poly(cis-butadiene) rubber blends*, J. Macromol. Sci. B: Phys. 44 (2005), pp. 651–664.
- [39] R.T.D. Prabhakaran, B.J. C. Babu, and V.P. Agrawal, *Quality modeling and analysis of polymer composite products*, Polym. Compos. 27 (2006), pp. 329–340.
- [40] D.V. Pleshakov, *Influence of network topology on mechanical properties of network polymers*, Mol. Simul. 31 (2005), pp. 999–1003.
- [41] Y. Yang, *Graph theory of viscoelastic and configurational properties of Gaussian chains*, Macromol. Theor. Simul. 7 (1998), pp. 521–549.
- [42] G. Gündüz, D. Erol, and N. Akkaş, *Mechanical properties of E-glass fiber reinforced polyester-isocyanate hybrid network composites*, J. Compos. Mater. 39 (2005), pp. 1577–1589.
- [43] G. Gündüz, G. Dikencik, M. Fares, and L. Aras, *Scaling relations in weak and late cross linked polymers*, J. Phys. Condens. Matter 14 (2002), pp. 2309–2322.
- [44] R.B. Seymour and C.E. Carraker, Jr., *Structure–Property Relations in Polymers*, Plenum Press, New York/London, 1984.
- [45] I. Jacqueline and H.G. Mary, *Encyclopedia of Chemical Technology*, 4th ed., Wiley, New York, NY, 1997, pp. 370–389.
- [46] J. Brandrup and E.H. Immergut, *Polymer Handbook*, Wiley, New York, 1989.
- [47] Y. Shimura, *Effects of composition on solution properties of styrene-acrylonitrile copolymers*, J. Polym. Sci. A4 (1966), p. 423.
- [48] G. Gündüz and G. Dikencik, *Temperature dependence of hardness of weakly crosslinked poly (methyl methacrylate) network formed by late addition of the crosslinker*, Chem. Eng. Commun. 193 (2006), pp. 526–535.

- [49] C.R. Bohn, J.R. Schaefgen, and W.O. Statton, *Laterally ordered polymers – polyacrylonitrile and poly(vinyl trifluoroacetate)*, J. Polym. Sci. 55 (1961), pp. 531–549.
- [50] A.M. Saum, *Intermolecular association in organic nitriles – the CN dipole-pair bond*, J. Polym. Sci. 42 (1960), pp. 57–66.
- [51] M.A. Dalin, I.K. Kolchin, and B.R. Serebryakov, *Acrylonitrile*, Technomic Publication, Westport, CT, 1971.
- [52] L.E. Wolfram, J.G. Grasselli, and J.L. Koenig, Appl. Polym. Symp. (25) (1974), pp. 27–40.
- [53] J. Gross and J. Yellen, *Graph Theory and Its Applications*, CRC Press, Boca Raton, FL, 1999.
- [54] G. Gündüz and M. Kirkin, *Hardness of weakly and late crosslinked polymethylmethacrylate and its relation to chain statistics*, Fundamentals of Polymers, Polym. Int. 35 (1994), pp. 61–65.
- [55] A. Kumar and R.K. Gupta, *Fundamentals of Polymers*, McGraw-Hill, New York, 1998, p. 147.
- [56] P.J. Flory, *Principles of Polymer Chemistry*, Cornell University Press, Ithaca, NY, 1957.
- [57] H. Wiener, *Structural determination of paraffin boiling points*, J. Am. Chem. Soc. 69 (1947), pp. 17–20.
- [58] H. Hosoya, *Topological index, a newly proposed quantity characterizing the topological nature of structural isomers of saturated hydrocarbons*, Bull. Chem. Soc. Jpn 44 (1971), pp. 2332–2339.
- [59] M. Randic, *On characterization of molecular branching*, J. Am. Chem. Soc. 97 (1975), pp. 6609–6615.
- [60] A.T. Balaban, *Highly discriminating distance-based topological index*, Chem. Phys. Lett. 89(5) (1982), pp. 399–404.
- [61] H.P. Schultz, *Topological organic chemistry 1: graph theory and topological indices of alkanes*, J. Chem. Inf. Comput. Sci. 29 (1989), pp. 227–228.
- [62] L. Pogliani, *Modeling with semiempirical molecular connectivity terms*, J. Phys. Chem. A (103) (1999), pp. 1598–1610.
- [63] D. Amic, D. Beslo, B. Lucic, S. Nikolic, and N. Trinajstić, *The vertex-connectivity index revisited*, J. Chem. Inf. Comput. Sci. 38 (1998), pp. 819–822.
- [64] E. Estrada, *Edge adjacency relationships and a novel topological index related to molecular volume*, J. Chem. Inf. Comput. Sci. 35 (1995), pp. 31–33.
- [65] F. Yang, Z.D. Wang, Y.P. Huang and H.L. Zhu, *Novel topological index F based on incidence matrix*, J. Comput. Chem. 24 (2003), pp. 1812–1820.
- [66] A.G. Saliner and X. Girones, *Topological quantum similarity measures: applications in QSAR*, J. Mol. Str. Theochem. 727 (2005), pp. 97–106.
- [67] D.J. Klein, J.L. Palacios, and N. Trinajstić, *Random walks and chemical graph theory*, J. Chem. Inf. Comput. Sci. 44 (2004), pp. 1521–1525.
- [68] Q.N. Hu, Y.Z. Liang, X.L. Peng, H. Yin, and K.T. Fang, *Structural interpretation of a topological index, 1: external factor variable, connectivity index (EFVCI)*, J. Chem. Inf. Comput. Sci. 44 (2004), pp. 437–446.
- [69] I. Gutman, D. Vukicevic, and J. Zerovnik, *A class of modified Wiener indices*, Croat. Chem. Acta 77(1–2) (2004), pp. 103–109.
- [70] I. Gutman and N. Trinajstić, *Graph theory and molecular orbitals: total π -electron energy of alternant hydrocarbons*, Chem. Phys. Lett. 17(4) (1972), pp. 535–538.
- [71] G.P. McCauley and D.J. Thouless, *Evaluation of an integral in the theory of fluctuation free energy in terms of Euler paths round a graph*, J. Phys. F: Met. Phys. 6 (1976), pp. 109–113.
- [72] T.P. Radhakrishnan and W.C. Herndon, *Graph theoretical analysis of water clusters*, J. Phys. Chem. 95 (1991), pp. 10609–10617.
- [73] S. Markovic, *The evaluation of the 8th moment for benzenoid graphs*, Theor. Chim. Acta 81 (1992), pp. 237–244.
- [74] J.R. Dias, *Facile calculations of the characteristic polynomial and pi-energy levels of molecules using chemical graph-theory*, J. Chem. Educ. 64(3) (1987), pp. 213–216.
- [75] R. Simha and U. Yahsi, *Statistical thermodynamics of hydrocarbon fluids – scaling parameters and their group contributions*, J. Chem. Soc. Faraday Trans. 91(16) (1995), pp. 2443–2455.
- [76] K.J. Burch, *Boiling point models of alkanes*, Match 47 (2003), pp. 25–52.
- [77] E. Estrada, J.A.R. Velazquez, and M. Randic, *Atomic branching in molecules*, Int. J. Quantum Chem. 106 (2006), pp. 823–832.
- [78] L. Pogliani, *Model of the physical properties of halides with complete graph-based indices*, Int. J. Quantum Chem. 102 (2005), pp. 38–52.
- [79] A.A. Taherpour and F. Shafiei, *The structural relationship between Randic indices, adjacency matrixes, distance matrixes and maximum wave length of linear simple conjugated polyene compounds*, J. Mol. Struct.: Theochem 726 (2005), pp. 183–188.
- [80] M. Randic and S.C. Basak, *On use of the variable connectivity index (1chi(f) in QSAR: Toxicity of aliphatic ethers*, J. Chem. Inf. Comput. Sci. 41 (2001), pp. 614–618.
- [81] L. Pogliani, *Molecular connectivity model for determination of physicochemical properties of α -amino acids*, J. Phys. Chem. 97 (1993), pp. 6731–6736.
- [82] ———, *Molecular modeling by linear combinations of connectivity indexes*, J. Phys. Chem. 99 (1995), pp. 925–937.
- [83] G. Caporossi, I. Gutman, P. Hansen, and L. Pavlovic, *Graphs with maximum connectivity index*, Comp. Biol. Chem. 27 (2003), pp. 85–90.
- [84] J. Bicerano, *Prediction of Polymer Properties*, Marcel Dekker, Inc., New York, NY, Chapter 2, 1996.
- [85] S.J. Chen and K.A. Dill, *Statistical thermodynamics of double-stranded polymer molecules*, J. Chem. Phys. 103(13) (1995), pp. 5802–5813.
- [86] M.C.P. Van Eijk and F.A. M. Leermakers, *Semi-flexible polymers at a liquid-liquid interface: self-consistent field calculations*, J. Chem. Phys. 109(11) (1998), pp. 4592–4601.
- [87] P. Sozzani, M. Galimberti, and G. Balbontin, *Syndiotactic polypropylene after drawing – the effect of stretching polymer-chains on magic angle spinning NMR*, Makromol. Chem. Rapid Commun. 13 (1992), pp. 305–310.
- [88] S.L. Huang and J.Y. Lai, *Structure-tensile properties of polyurethanes*, Eur. Polym. J. 33 (1997), pp. 1563–1567.

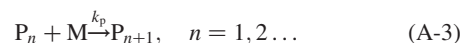
Appendix A. Mathematical modelling

In radical polymerisation, the initiator molecules (I_2) slowly decompose and the chains form instantly from monomers M. The chains terminate by transfer, coupling, or disproportionation. We can show the steps by,

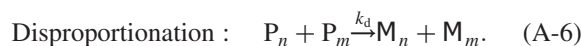
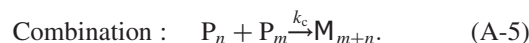
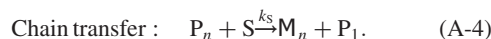
Initiation:



Propagation:



Termination:



In termination step, chain transfer and combination reactions result in dead and/or inactive polymer chains. In disproportionation, one chain becomes dead and the other inactive, that is, it ends up with a vinyl group.

The rate of initiation (r_i) can be written from Equation (A-2) as follows,

$$r_i = k_1[I][M], \quad (\text{A-7})$$

where $[I]$ is the concentration of the initiator radical and $[M]$ is the concentration of the monomer. The rate of propagation (r_p) can be written from Equation (A-3) as follows,

$$r_p = -k_1[I][M] - k_p[M][\lambda], \quad (\text{A-8})$$

where λ is the total concentration of growing polymer radicals (i.e. $\lambda = \sum_{n=1}^{\infty} [P_n]$). Since $[M] \gg [\lambda] \gg [I]$, Equation (A-8) can be approximated by,

$$r_p \approx -k_p[M][\lambda]. \quad (\text{A-9})$$

The termination rate (r_t) can be written as,

$$r_t = k_t \lambda^2, \quad (\text{A-10})$$

where termination takes place between two radicals.

The kinetic chain length ν is defined as the average number of monomer molecules reacting with a polymer radical during the lifetime of the radical [55]. This will be the ratio of the consumption rate of monomer (i.e. r_p) to the rate of generation of polymer radicals, that is,

$$\nu = \frac{r_p}{r_i}. \quad (\text{A-11})$$

According to quasi steady state approximation, the rate of initiation can be assumed to be equal to the rate of termination, that is, $r_i \approx r_t$. So Equation (A-11) becomes,

$$\nu = \frac{r_p}{r_i} = \frac{r_p}{r_t} = \frac{k_p[M][\lambda]}{k_t[\lambda]^2} = \frac{k_p[M]}{k_t[\lambda]}, \quad (\text{A-12})$$

where Equations (A-9) and (A-10) were substituted in.

The rate for the radicals can be written down from Equations (A-2), (A-5) and (A-6) such that,

$$\frac{d\lambda}{dt} = \frac{1}{dt} \sum_{n=1}^{\infty} [P_n] = k_1[I][M] - k_{tc}\lambda^2 - k_{td}\lambda^2 = 0, \quad (\text{A-13})$$

where k_{tc} and k_{td} are the termination rate constants by coupling and disproportionation, respectively. The chain transfer was neglected in Equation (A-13). The λ (i.e. a radical) is an intermediate compound. The steady-state approximation of chemical kinetics implies that $d\lambda/dt \rightarrow 0$. From Equation (A-13), one gets,

$$\lambda_p = \left[\frac{k_1}{k_t} [I][M] \right]^{1/2}, \quad (\text{A-14})$$

where $k_t = k_{tc} + k_{td}$.

The rate equation for $[I]$ can be found from Equations (A-1) and (A-2), such that,

$$r_i = 2k_0[I_2] - k_1[I][M]. \quad (\text{A-15})$$

This rate can also be set equal to zero according to steady state approximation because $[I]$ is an intermediate. Equation (A-15)

then gives,

$$[I] = \frac{2k_0[I_2]}{k_1[M]}. \quad (\text{A-16})$$

This equation is substituted in Equation (A-14), which is then substituted in Equation (A-12). It then gives,

$$M = \kappa \frac{[M]}{[I_2]^{1/2}}. \quad (\text{A-17})$$

Since there is a one-to-one correspondence between the kinetic chain length ν and the molecular weight of the polymer M , ν was substituted by M in Equation (A-17), where κ takes care of all the constants. It is seen from Equation (A-17) that the chain length decreases with the concentration of the initiator. The initiator concentration continuously decreases during the course of polymerisation. Therefore, chain length is expected to increase with time in the course of polymerisation because there would be less number of growing chains so their termination with coupling or disproportionation would be difficult. However, the concentration of the monomer (e.g. M) decreases in time. Therefore, the change of the molecular weight of the polymer (e.g. M) in time depends on the relative effects the concentrations of the monomer and of the initiator. Other effects such as reactivation of the vinyl-terminated inactive chains, and auto-acceleration are not considered in the above arguments. When a vinyl-terminated linear chain is activated with a polymer radical then a branched chain forms with highly increased molecular weight. As the concentration of vinyl-terminated chains increase in time, the molecular weight of chains also increases in time. Another effect that increases the molecular weight is so-called auto-acceleration effect. When the viscosity of the medium increased due to the accumulation of polymer chains, the diffusion of chains become difficult and termination is suppressed. But the radical chains keep growing because monomers diffuse and react with the somehow stationary chain radical. This effect is called auto-acceleration.

In cross-linked polymerisation, if the cross-linker is more reactive than the monomer then it is depleted at a faster rate and the chain lengths between two cross-linking sites or the loop sizes increase further in the course of polymerisation. So it is seen that (i) the decay rate constant of the initiator, (ii) the polymerisation rate constants which influence the monomer concentration M , (iii) the reactivity of the cross-linker and also (iv) the concentration of the cross-linker all influence the rigidity of the network formed and thus the hardness of the network polymer. The first three of these depends on the chemical structure and temperature. The fourth one can be fixed experimentally. In order to work on the dependence of hardness on the distribution of chain lengths between two cross-linking sites, we must experimentally change the molecular weight. This can be done by the late addition of the cross-linker. Suppose we have added the cross-linker some time after the start of the polymerisation. We get linear polymers until the cross-linker is added, and then on, we get cross-linked polymer. So the final product is a kind of interpenetrating polymer of the linear chains and the cross-linked network. The hardness of the polymer mostly depends on soft segments, which lowers hardness, and the polymer is expected to exhibit a decreasing

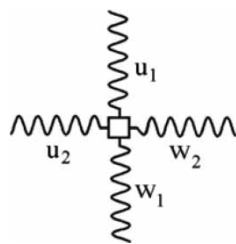


Figure A-3. Incoming (u_1 and u_2) and outgoing (w_1 and w_2) chains at the cross-linker which is shown by the small square.

backbone. The radical forms and terminates in a few fraction of a second. The second step shows the reaction between a radical and an inactive chain which has y number of monomer units on its backbone. It results in a branched chain on further propagation. In the presence of cross-linker in the medium, the cross-linker can attach to z' -chain, or it may attach to the branched chain. In the last reaction of Figure A-2, the branched chain radical reacts with another z'' number of monomers and then reacts with the cross-linker.

Let C be the mole fraction of the cross-linker. Thus the probability of a radical to react with a monomer becomes proportional to $1 - C$, and the probability to achieve u new units is equal to $(1 - C)^u$. The probability then to react with a cross-linker is $(1 - C)^u C$. A cross-linker molecule emanates four arms, two incoming and two outgoing. So the probability of addition of two new z_1 and z_2 units in the form of outgoing chains is equal to,

$$P = (1 - C)^{u_1} (1 - C)^{u_2} C^2, \quad (\text{A-18})$$

or,

$$P = (1 - C)^u C^2, \quad (\text{A-19})$$

where

$$u = u_1 + u_2. \quad (\text{A-20})$$

Note that,

$$u = y + z. \quad (\text{A-21})$$

Assume that the cross-linker attaches to two chains u_1 and u_2 , and then two new chains emanate from it with w_1 and w_2 monomer units as seen from Figure A-3.

Let x_1 and x_2 be the total number of units, such that,

$$u_1 + w_1 = x_1, \quad (\text{A-22})$$

$$u_2 + w_2 = x_2. \quad (\text{A-23})$$

The u -chains which form before the reaction with the cross-linker, and w -chains which contain a cross-linker molecule at the backbone both display chain length distributions. Any chain length distribution can be identified by its most probable and/or by its average values [56]. In other words, y -chains, z -chains, u -chains and w -chains all can be described separately by distribution functions though there is no easy way, probably no way, to determine the distribution of z -, u -, and w -chains

experimentally. The distributions of these chains can be simply related to each other through a constant, such that,

$$y = k_1 z = k_2 u = k_3 w, \quad (\text{A-24})$$

where k_1 is a ratio of the maximum or the average value of the y - and z -chain length distributions; k_2/k_1 is of z - and u -chain distributions, and k_3/k_2 is of u - and w -chain distributions, respectively. Equations (A-22) and (A-23) can be generally written as,

$$u + w = x. \quad (\text{A-25})$$

Equations (A-24) and (A-25) then gives,

$$\begin{aligned} \frac{y}{k_2} + \frac{y}{k_3} &= \left(\frac{1}{k_2} + \frac{1}{k_3} \right) y = k_4 y = x, \\ u = \frac{y}{k_2} &= \frac{x}{k_2 k_4} = k' x. \end{aligned} \quad (\text{A-26})$$

In this equation, two branches of the cross-linker (i.e. in and out) are considered. This equation can be written also in terms of the number of linkages. There are two crossing chains at the cross-linker. Each chain has one less linkage than the number of monomer units on the chain. So, we should subtract '2' from the right hand side of Equation (A-26), such that,

$$u = k' x - 2. \quad (\text{A-27})$$

We could treat w_1 and w_2 chains separately and then add them up as was done in the former work [43]. However, we would end up with the same result.

Equation (A-19) now takes the form,

$$P = (1 - C)^{k'x-2} C^2. \quad (\text{A-28})$$

The product of Equation (A-28) and the number of combinations of u s that fulfill Equation (A-27) gives the probability that $k'x$ units distribute over two linear chains emanating from the cross-linker. Therefore,

$$P \sim \left[\frac{(k'x)!}{(k'x-2)!} \right] (1 - C)^{k'x-2} C^2. \quad (\text{A-29})$$

The factor $(k'x)!/(k'x-2)!$ is the permutation showing in how many number of ways the cross-linker and the monomer can interact with the chain. It denotes the probability of the arrangements of monomer molecules and cross-linker on the chain.

Equation (A-29) simplifies to,

$$P \sim (k'x)(k'x-1)(1 - C)^{k'x-2} C^2. \quad (\text{A-30})$$

As mentioned earlier, the experimental determination of the distribution or the average molecular weight of z -, u - and w -chains is either impossible or extremely difficult with the known techniques. However, there exists a relation between u and x given by Equation (A-26) in terms of the number of monomer units, and by Equation (A-27) in terms of the number of linkages. y can be determined as the molecular weight of linear chains already formed just before the addition of the

cross-linker. Since a simple relation exists between y and u , and between u and x as seen from Equations (A-24) and (A-26), we can write,

$$u = k'x = \frac{y}{k_2} = kM, \quad (\text{A-31})$$

where we have substituted the number of monomer units y on the prepolymer by the molecular weight of the prepolymer M . Equation (A-30) now becomes,

$$P \sim (kM)(kM - 1)(1 - C)^{kM-2}C^2. \quad (\text{A-32})$$

The chain configuration of the network formed due to the late addition of the cross-linker obeys a distribution given by Equation (A-30) or (A-32).

Now we can introduce graph-theoretical concepts to transform Equation (A-32) into a hardness equation. The chemical application of graph theory was pioneered by Wiener [57] five decades ago, but its importance was realised two or three decades later. He introduced so-called 'structural variable', and showed that the boiling points of alkanes could be correlated with structure by means of a theoretical equation. Wiener's approach was the first use of graph theory to explain the physicochemical properties of molecules, and the key tool of his analysis today known as the 'Wiener index' is defined as the sum of distances between all pairs of vertices. Later, new indices were defined such as the Hosoya index [58], the Randic index [59], the Balaban index [60], the Schultz index [61], etc. [62–69]. Graph theory is a useful tool when the properties of molecules depend on its topology. In this respect, it can be applied to analyze structure–property modelling, as well as chemical reactions [70–83]. It finds similar applications also in polymers [20–41,84–86]. The basic assumption in the use of graph theory is that the molecular motions such as vibration, rotation and electronic excitation are affected by the neighboring atom in the structure. In a short linear chain such as a short polyethylene chain all the atoms (i.e. carbon atoms) on the backbone except the end atoms display similar behaviour, and thus yield similar eigenvalues when the differential equations of vibrations are solved. The branching introduces a break down of the similarity (or symmetry), and it can be taken into account by using the appropriate topological indices mentioned above.

In long chains, we have additional modes of motions due to conformations and configurations. For instance, long chains entangle, and the molecular motions of the backbone atoms nearby the entanglement sites are different than those far away from these sites. The same is true also for cross-linked polymers. A short chain between two cross-linking sites is not much free, and looks like a tight string between two hooks, while a long chain is like a loose string. The backbone atoms of a short tight chain between the cross-linking sites thus have smaller displacements, and rotations. In contrast, the atoms of a long free linear chain can easily make larger displacements and rotations. In addition, chain slip is likely to occur in long linear chains. In terms of viscoelasticity, the long linear chains are likely to display both spring and dashpot behaviour, while the short tight chains between the cross-linking sites mostly display spring behaviour. Similarly, the spring behaviour is enhanced in

linear chains if there is high entanglement density. The long chains between the cross-linking sites as in weakly cross-linked polymers naturally exhibit both spring and dashpot behaviour at varying proportions depending on the length of the chain. In interpenetrating systems as in our case linear chains can make entanglements with the chains of cross-linked polymers also. So whether we have linear or cross-linked polymers, the chain length between the entanglement or cross-linking sites determines the relative extents of spring or dashpot behaviour. There have been different studies in the literature about the change of chain conformations under load. Sozzani et al. reported that *st*-polypropylene chains became oriented on stretching and trans-gauge ratio shifted in favour of *trans*. In the necking region of deformation *tggt* and *gttg* switched to *tttt* [87]. Huang and Lai showed that interchain hydrogen bonding in polyurethanes decreased with increasing strain [88].

In our system, there are two parameters which control the chain length; one is the molecular weight of the prepolymer and the other the concentration of the cross-linker. Equation (A-32) actually involves only these two parameters. Since the mechanical strength or the hardness in our case depends on the extent of spring and dashpot properties of polymer, we can simply conclude that hardness depends on the length of chains and also on the number of cross-linking sites in a unit volume. As mentioned earlier, in graph theoretical interpretation the cross-linking or entanglement site naturally corresponds to 'vertex', and the chain length between these sites corresponds to 'edge'. However, the entanglement points may move while the cross-linking sites are stationary, i.e. the former is non-affine while the other is affine connection under any mechanical distortion. Therefore, their contributions to hardness are different. Nevertheless, the entanglement density in a unit volume is controlled by the molecular weight of the prepolymer and also by the concentration of the cross-linker. In other words, the entanglement density correlates with these two parameters. So the change in hardness can be written as follows by using Equation (A-32),

$$\Delta H = h(kM)(kM - 1)(1 - C)^{kM-2}C^2, \quad (\text{A-33})$$

where H denotes the hardness of the polymer, ΔH denotes the change in hardness. h is a constant coefficient with the physical unit of hardness. Since the probability distribution is based on the late addition of the cross-linker, the hardness of the network polymer can be written as,

$$H = h_0 + \Delta H, \quad (\text{A-34})$$

where h_0 is the hardness of the polymer when the cross-linker is added just at the very beginning, where there is no polymerisation and the molecular weight of chain is that of monomer only. From Equations (A-33) and (A-34),

$$H = h_0 + h(kM)(kM - 1)(1 - C)^{kM-2}C^2. \quad (\text{A-35})$$

As the polymerisation keeps going, there would be an increase in the number of polymer chains formed. Some of these chains are partly vinyl-terminated but inactive and some are completely dead without any vinyl functional group. So the system discussed here is actually a kind of interpenetrating

polymer system where linear chains interpenetrate the weakly cross-linked system. In very late additions of the cross-linker, there would be an increased number of linear chains either in the form of dead chains or vinyl-terminated inactive chains. These chains would necessarily soften the structure. This affect is not apparently seen in Equation (A-35), because, the probability equation is based only on the network formed. Nevertheless, the probability equation works in both directions

taking into account both linear and cross-linked chains. Because, the increase in the molecular weight of the prepolymer (e.g. M) is a time dependent process, and the number of dead and inactive chains and their molecular weights also increase with time. All parameters go in parallel, and they are all correlated. Therefore, if the influence of the probability function on hardness decreases then the influence of linear chains on hardness increases, or vice versa.